Materials Advances

ROYAL SOCIETY OF CHEMISTRY

COMMUNICATION

View Article Online
View Journal | View Issue

Open Access Article. Published on 14 april 2023. Downloaded on 4-2-2026 12:17:45.
This article is licensed under a Creative Commons Attribution 3.0 Unported Licence.

Check for updates

Cite this: *Mater. Adv.*, 2023, **4**, 4344

Received 31st December 2022, Accepted 2nd April 2023

DOI: 10.1039/d2ma01106a

rsc.li/materials-advances

Eco-friendly Egyptian blue ($CaCuSi_4O_{10}$) dye for luminescent solar concentrator applications

Tharmakularasa Rajaramanan,[ac] Mansoureh Keykhaei,[a] Fatemeh Heidari Gourji,[a] Punniamoorthy Ravirajan,[c] Meena Senthilnanthanan,[d] Øyvind Frette[b] and Dhayalan Velauthapillai *[a]

This study focuses on synthesizing the heavy metal-free ancient Egyptian blue (EB; $CaCuSi_4O_{10}$) dye using a facile ceramic method for luminescent solar concentrator (LSC) application. XRD, SEM and EDX results confirmed that this well-crystallized material is successfully synthesized. Optical studies revealed that EB has a high Stokes shift and possesses an average lifetime of 110.50 μs with a quantum yield of 12.93%. Finally, an EB-integrated LSC was fabricated that exhibits a power conversion efficiency (η) of 0.15% and an optical conversion efficiency (η_{opt}) of 1.21%, which are the highest values reported so far using EB.

1. Introduction

One of the constraints with electricity production using conventional Si-based solar cells is the amount of area that is needed for roof-top or stand-alone installations.[1] The lack of flexibility and weight are other challenges that must be addressed to ensure affordable energy for all (*i.e.*, Sustainable Development Goal 7) based on solar cell technologies.[2] Lots of research into solar cells has been focused on novel materials and new processes for solar cell fabrication. Luminescent solar concentrators (LSCs) have been explored as a potential solution to tackle the aforementioned limitations. A typical LSC consists of a transparent glass plate, which is coated with a highly luminescent material that absorbs solar radiation. These materials then re-emit the absorbed photons at long wavelengths which are transported to the edges of the LSCs that are coupled with the solar cell, thus producing electricity.[3,4] LSCs serving as semitransparent photovoltaic windows could become an important element in net-zero-energy-consumption buildings of the future.[5] Such laminated glass offers benefits towards security, soundproofing and energy conservation through the building of windows, facades, and transparent roofs.[6,7] In addition, an LSC does not require solar tracking and can operate in both diffuse and direct sunlight.[6] Nevertheless, LSC development faces various challenges, many of which are related to the materials used in its design. Luminescent materials can be either organic or inorganic.[8–11] The major inorganic luminescent materials are quantum dots (QDs) and rare-earth (RE)-based luminescent materials, where each type possesses its own benefits and drawbacks, making neither of them an ideal LSC candidate.[12] Organic luminescent dyes typically suffer from large self-absorption losses (a large overlap between the absorption and emission spectra), poor stability, narrow-band absorbance, and a lack of spectral matching with the peak external quantum efficiency (EQE) of the solar cells.

Egyptian blue (EB) is a luminescent material that is also called cuprorivaite ($CaCuSi_4O_{10}$). It is a copper-based dye and can overcome the limitations of toxicity and cost-related issues that are seen with other luminescent materials.

It has superior stability and was produced by ancient chemists as a pigment (Fig. 1), which shows luminescent abilities even after

Fig. 1 Ancient painting in ceiling reliefs in the Hathor Temple in Qena, Egypt (Source: https://www.chemistryworld.com/features/egyptian-blue-more-than-just-a-colour/9001.article)

[a] Faculty of Engineering and Science, Western Norway University of Applied Sciences, P.O. Box 7030, 5020 Bergen, Norway. E-mail: Dhayalan.Velauthapillai@hvl.no
[b] Department of Physics and Technology, University of Bergen, Allegaten 55, 5007 Bergen, Norway
[c] Clean Energy Research Laboratory, Department of Physics, University of Jaffna, Jaffna 40000, Sri Lanka
[d] Department of Chemistry, University of Jaffna, Jaffna 40000, Sri Lanka

© 2023 The Author(s). Published by the Royal Society of Chemistry

Open Access Article. Published on 14 april 2023. Downloaded on 4-2-2026 12:17:45.
This article is licensed under a Creative Commons Attribution 3.0 Unported Licence.

several thousand years.[13] Moreover, it is a red-light-emitting phosphorescent substance, which shows the highest quantum efficiency in the near-infrared (NIR) spectral range (800–1100 nm). The Stokes shift for this material is as high as 280 nm, which minimizes re-absorption events.[14] In addition, silicon solar cells have the ability to absorb in the NIR range at wavelengths around 1000 nm; however, the solar spectrum itself shows a deficiency at such wavelengths after the radiation has passed through the atmosphere.[15] Considering all these factors, we have developed a novel, efficient and cost effective LSC based on a stable and non-toxic artificial pigment with a PL peak at ∼900 nm, which matches well with the peak EQE of crystalline silicon (c-Si) solar cells (∼850–950 nm).

2. Materials and method

The $CaCuSi_4O_{10}$ dye was synthesized using a modified procedure adopted from elsewhere.[14] $CaCO_3$ (0.66 g, 99+%, Acros Organics), SiO_2 (1.59 g, 99.5%, Alfa Aesar), Cu_2CO_3 (0.73 g, 54–56% Cu, Acros Organics), Na_2CO_3 (0.18 g, 99.95%, Acros Organics), NaCl (0.06 g, ≥99.0%, Sigma-Aldrich), and $Na_2B_4O_7$ (0.125 g, anhydrous powder, Alfa Aesar) were ground well using mortar and pestle to form a homogeneous mixture. Then, the mixture was transferred into a ceramic dish and heated at a high temperature of around 900 °C for 16 hours in a muffle furnace. After cooling to room temperature, the product was washed with aqueous HCl ($HCl:H_2O$ = 70:30) to get rid of residues. Finally, the product was washed several times with DI-water to remove the acid, and subsequently dried at 60 °C overnight in an oven (Fig. 2). The synthesized $CaCuSi_4O_{10}$ and polyvinylpyrrolidone (a binder; average MW 3500, K12, Acros Organics) were mixed well using a mortar and pestle. Then, the mixture was dispersed in 20 mL of ethanol solvent. Finally, the dispersed mixture was coated onto a quartz glass surface at 100 °C on a hot plate *via* spray coating.

3. Results and discussion

3.1. Structural characterization of Egyptian blue

XRD measurements were carried out to confirm the crystal structure of the Egyptian blue using a D8 ADVANCE ECO diffractometer with a 1 kW copper X-ray tube with the scan range of 10–90° (2θ). As displayed in Fig. 3a, significant sharp peaks of cuprorivaite ($CaCuSi_4O_{10}$) were detected along with a small amount of quartz.[16] The presence of the quartz (SiO_2) impurity could be attributed to the un-reacted SiO_2 precursor. All of the observed major peaks matched very well with the literature, confirming the formation of the target material. The morphology and elemental composition of the prepared material were studied using a scanning electron microscope (FESEM, Jeol JSM-7400F) along with an energy-dispersive X-ray spectrometer (EDX). Prior to the analysis, the material was ground well using a mortar and pestle to form a smooth powder. The results show that many of the particles possess irregular shapes of 1–10 μm size while some are in the nano size range (Fig. 3b). The EDX spectra (Fig. 3c) showed clear peaks for calcium, copper, silicon, and oxygen elements, which confirmed the structure of EB. Furthermore, EDX mapping illustrated the extensive dispersion of the elements in the material, which suggests that all the elements are uniformly distributed in the synthesized material (Fig. 3d).

3.2. Optical characterization of Egyptian blue

The optical properties of the material were thoroughly studied using an FS5 spectrofluorometer. The PL excitation and emission

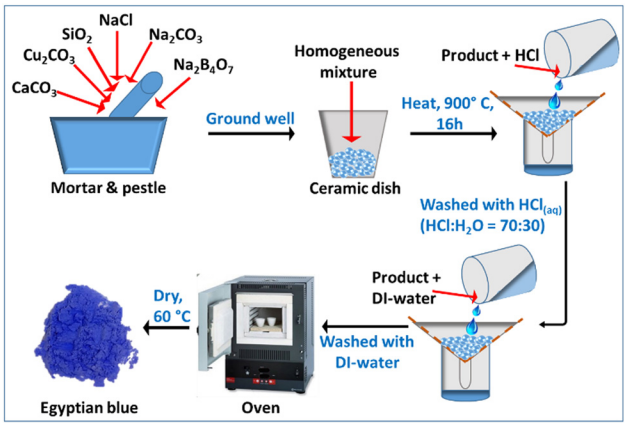

Fig. 2 Schematic diagram of the synthesis of Egyptian blue.

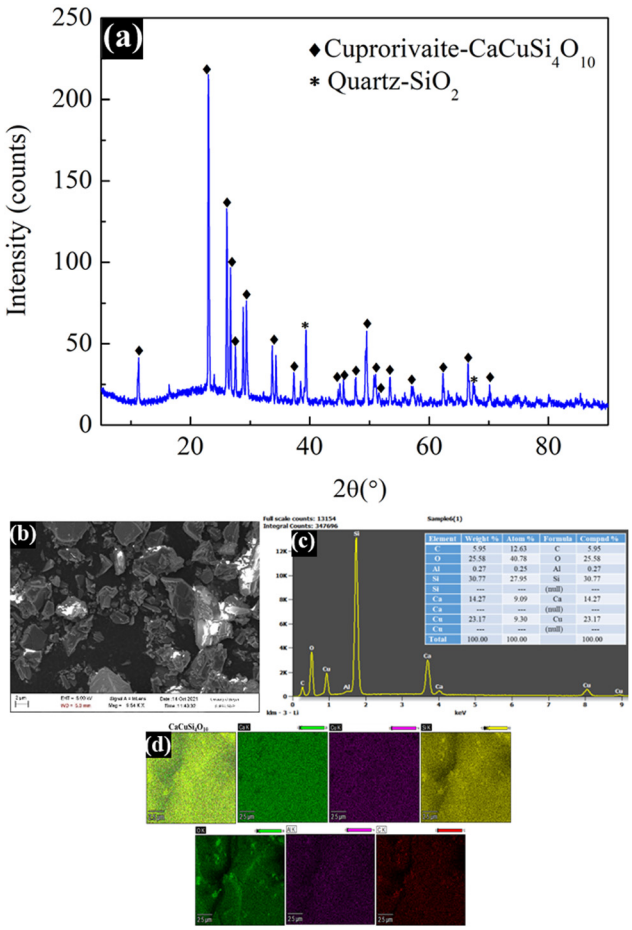

Fig. 3 XRD (a), SEM (b), EDX (c), and EDX mapping (d) images of the synthesized Egyptian blue.

Open Access Article. Published on 14 april 2023. Downloaded on 4-2-2026 12:17:45.
This article is licensed under a Creative Commons Attribution 3.0 Unported Licence.

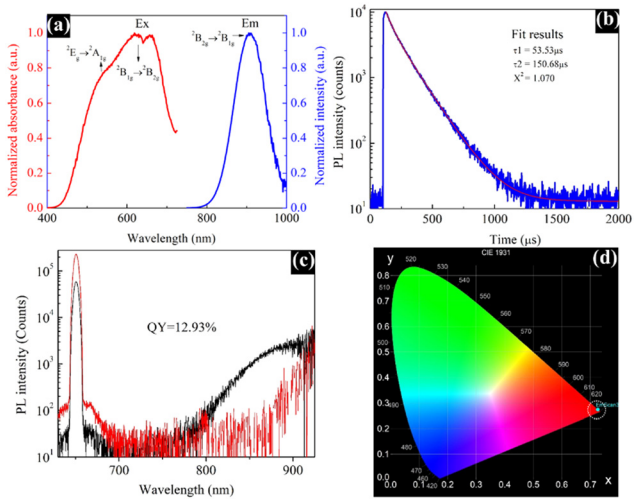

Fig. 4 PL excitation and emission spectra (a), PL decay curve (b), PL quantum yield measurement (c), and CIE chromaticity diagram (d) of the Egyptian blue.

spectra were measured in the spectral range from 400 to 1000 nm. As illustrated in Fig. 4a, the maximum PL excitation, monitored at 635 nm, corresponding to the $^2B_{1g} \rightarrow {}^2B_{2g}$ and $^2E_g \rightarrow {}^2A_{1g}$ electronic transitions can be attributed to Cu^{2+} ions, which are the photoluminescent component in the EB. The maximum emission displayed at 909 nm is related to the $^2B_{2g} \rightarrow {}^2B_{1g}$ electronic transition.[17] Moreover, EB possesses a large Stokes shift, due to which re-absorption losses are minimized, and the emission at 909 nm matches well with the photo-responsive region of silicon solar cells; all these observations make this dye well-suited for LSC application. The PL decay curve in Fig. 4b does not match well with a single exponential decay; hence, a bi-exponential decay curve fitting method was employed. The obtained results are T_1 = 53.53 μs, T_2 = 150.68 μs and X^2 = 1.070.

Moreover, the EB dye showed an average lifetime of 110.50 μs. Earlier, Comelli *et al.* reported mono-exponential decay kinetics with a lifetime of 138 μs for EB, which is reasonably similar to our findings.[18] The PL quantum yield measurements are displayed in Fig. 4c, which were obtained during the excitation and luminescence ranges of 640–660 and 798–914 nm, respectively. The synthesized EB dye exhibited a quantum yield of 12.93%, which is the highest value ever reported for the EB dye obtained *via* different synthetic routes.[14,17] Generally, the luminescence colour of any phosphorescent material can be illustrated using colour coordinates. Fig. 4d shows the CIE (Commission international de l'éclairage) chromaticity image of the EB dye. The synthesized material exhibited a maximum emission intensity with the CIE colour coordinates of (0.72, 0.27), which is close to the National Television System Committee (NTSC) red colour[19] as it is a red-emitting phosphorescent material.

3.3. Photovoltaic properties of an Egyptian blue-integrated luminescent solar concentrator

Fig. 5a displays the fabricated LSC integrated with the synthesized blue pigment dye, and Fig. 5b depicts the UV-vis transmittance spectrum of the same LSC plate, where the transmittance of the EB-coated LSC plate is compared with a bare (un-coated) quartz plate as a reference. This spectrum reveals that the glass is still transparent even after being coated with EB. The PV performance of the EB-coated LSC was analyzed, where a commercial silicon solar cell with an area of 4.0 cm^2 was edged onto the said LSC, and the results are shown in Fig. 5c and d. Solar cells of the same size were employed to record the measurements, and the *I–V* measurements were obtained under a light intensity of 1 Sun illumination using an AM 1.5G filter. All measurements were performed using a dark background, without the use of a reflective mirror/foil or a scattering background to reflect the photons that are emitted outside the escape cone back into the waveguide for recycling.

The power conversion efficiency (η) of the fabricated LSC was calculated using the following equation,[3] and the results are summarized in Table 1:

$$\text{PCE } (\eta) = I_{LSC} \times V_{OC} \times \text{FF}/(P \times A_{LSC})$$

where I_{LSC} is the short circuit current, V_{OC} is the open circuit voltage, FF is the fill factor of the PV cell attached to the LSC, P is the irradiation intensity, and A_{LSC} is the area of the LSC.

The optical conversion efficiency (η_{opt}) of the fabricated LSC was calculated using the following equation:

$$\eta_{opt} = I_{LSC}/(I_{cell} \times G)$$

where I_{cell} is the short-circuit current from the silicon solar cell under direct illumination, I_{LSC} is the short-circuit current from the LSC, and G is the geometric factor of the LSC. Currently, a standard protocol for determining the G factor value is not available within the research community, although the G factor plays a crucial role in determining the η_{opt}. In the literature, calculation of the G value has been reported either as the ratio

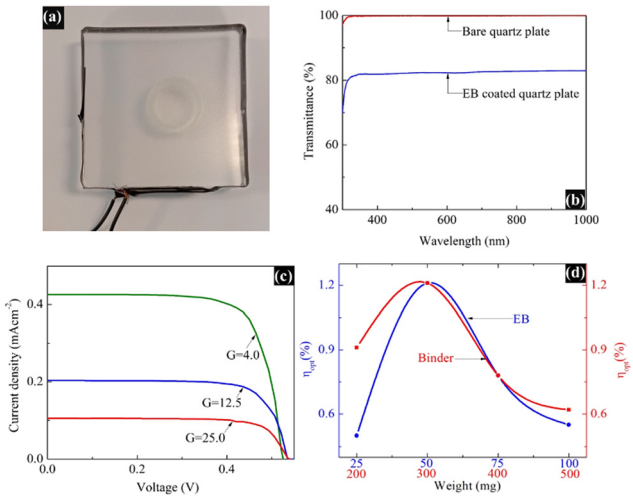

Fig. 5 Fabricated luminescent solar concentrator (10 × 10) integrated with Egyptian blue (a), UV-vis transmittance spectrum of the same LSC plate (b), photovoltaic performance of the LSC with different G factor values (EB, 50 mg; binder, 300 mg) (c), and variation of the optical efficiency with different amounts of EB (blue line, where 300 mg of binder was used and G = 4) and binder (red line, where 50 mg of EB was used and G = 4) (d).

 © 2023 The Author(s). Published by the Royal Society of Chemistry

Open Access Article. Published on 14 april 2023. Downloaded on 4-2-2026 12:17:45.
This article is licensed under a Creative Commons Attribution 3.0 Unported Licence.

Table 1 Summarized PV parameters of the fabricated LSC with different G values (EB, 50 mg; binder, 300 mg)

I_{LSC} (mA)	A_{LSC} (cm^2)	J_{LSC} (mA cm^{-2})	V_{OC} (V)	FF	η (%)	G	η_{opt} (%)
6.8	16	0.43	0.52	0.74	0.15	4.0	1.21
9.9	49	0.20	0.53	0.74	0.07	12.5	0.56
10.0	100	0.10	0.53	0.74	0.04	25.0	0.28

between the LSC front area and the solar cell area or as the ratio between the LSC front area and the total summed area of the edges of the LSC.[20,21] We calculate the G value using the ratio between the LSC front area and the solar cell area. In our study, the fabricated LSC with optimum amounts of EB and the binder exhibited maximum η and η_{opt} values for G = 4. No change in the V_{OC} and FF values was observed with an increase in the G value. The fabricated LSC with an active area of 16 cm^2 (G = 4) exhibited a short-circuit current (I_{LSC}) of 6.8 mA, a short circuit current density (J_{LSC}) of 0.43 mA cm^{-2}, an open-circuit voltage (V_{OC}) of 0.52 V and a fill factor (FF) of 0.74. When the silicon solar cell was directly exposed to 1 Sun illumination light, it showed I_{cell} = 140.0 mA, J_{cell} = 35.13 mA cm^{-2}, V_{OC} = 0.61 V and FF = 0.69. The calculated maximum η and η_{opt} values for the fabricated LSC are 0.15% and 1.21%, respectively.

Furthermore, the practical application of the fabricated LSC was demonstrated by connecting the device to a mini-sized electric table fan (Fig. 6).

4. Conclusion

In this study, a novel method to fabricate LSCs using the ancient Egyptian blue dye ($CaCuSi_4O_{10}$) has been established. The EB dye was synthesized successfully using a facile ceramic method, and its formation was confirmed *via* XRD, SEM and EDX measurements. The dye exhibited PL excitation and emission maxima at 635 and 909 nm, respectively. The time-resolved PL decay spectrum showed bi-exponential emission behavior with an average lifetime of 110.50 μs. Moreover, it possessed a quantum yield of 12.93%. The EB dye-incorporated LSC exhibited an impressive η and η_{opt} of 0.15% and 1.21%, respectively. The above findings suggest that the EB dye can be a suitable material for integration with LSCs for industrial applications.

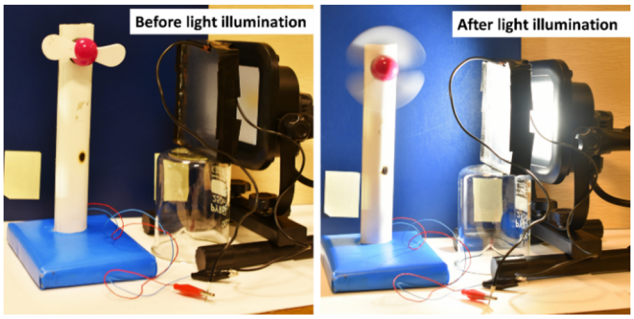

Fig. 6 Working model of the fabricated luminescent solar concentrator.

Author contributions

Tharmakularasa Rajaramanan: conceptualization, methodology, data curation, software, writing – original draft preparation. Mansoureh Keykhaei: conceptualization, methodology, data curation, reviewing and editing. Fatemeh Heidari Gourji: data curation, investigation, reviewing and editing. Punniamoorthy Ravirajan: data curation, investigation, validation, supervision, funding acquisition, reviewing and editing. Meena Senthilnanthanan: data curation, investigation, validation, supervision, reviewing and editing. Øyvind Frette: data curation, investigation, supervision. Dhayalan Velauthapillai: data curation, investigation, validation, supervision, visualization, funding acquisition, reviewing and editing.

Conflicts of interest

There are no conflicts to declare.

Acknowledgements

This research was funded by the Capacity Building and Establishment of a Research Consortium (CBERC) project, grant number LKA-3182-HRNCET and the Higher Education and Research collaboration on Nanomaterials for Clean Energy Technologies (HRNCET) project, grant number NORPART/2016/10,237. Open access funding provided by Western Norway University Of Applied Sciences.

References

1 T. Rajaramanan, G. R. A. Kumara, D. Velauthapillai, P. Ravirajan and M. Senthilnanthanan, *Mater. Sci. Semicond. Process.*, 2021, **135**, 106062.
2 D. McCollum, L. Gomez Echeverri, K. Riahi and S. Parkinson, SDG 7: ensure access to affordable, reliable, sustainable and modern energy for all, *A Guide to SDG Interactions: From Science to Implementation, International Council for Science*, International Council for Science, 2017, pp. 127–173.
3 Z. Li, X. Zhao, C. Huang and X. Gong, *J. Mater. Chem. C*, 2019, **7**, 12373–12387.
4 M. Cao, X. Zhao and X. Gong, *JACS Au*, 2023, **3**, 25–35.
5 F. Meinardi, H. McDaniel, F. Carulli, A. Colombo, K. A. Velizhanin, N. S. Makarov, R. Simonutti, V. I. Klimov and S. Brovelli, *Nat. Nanotechnol.*, 2015, **10**, 878–885.
6 M. K. Assadi, H. Hanaei, N. M. Mohamed, R. Saidur, S. Bakhoda, R. Bashiri and M. Moayedfar, *Appl. Phys. A: Mater. Sci. Process.*, 2016, **122**, 821.
7 J. Levitt and W. Weber, *Appl. Opt.*, 1977, **16**, 2684–2689.
8 J. Chen, H. Zhao, Z. Li, X. Zhao and X. Gong, *Energy Environ. Sci.*, 2022, **15**, 799–805.
9 X. Gong, H. Jiang, M. Cao, Z. Rao, X. Zhao and A. Vomiero, *Mater. Chem. Front.*, 2021, **5**, 4746–4755.
10 X. Gong, S. Zheng, X. Zhao and A. Vomiero, *Nano Energy*, 2022, **101**, 107617.
11 J. Li, H. Zhao, X. Zhao and X. Gong, *Nanoscale Horiz.*, 2023, **8**, 83–94.

Open Access Article. Published on 14 april 2023. Downloaded on 4-2-2026 12:17:45.
This article is licensed under a Creative Commons Attribution 3.0 Unported Licence.

12 W. G. Van Sark, K. W. Barnham, L. H. Slooff, A. J. Chatten, A. Büchtemann, A. Meyer, S. J. McCormack, R. Koole, D. J. Farrell and R. Bose, *Opt. Express*, 2008, **16**, 21773–21792.
13 P. García-Fernández, M. Moreno and J. A. Aramburu, *Inorg. Chem.*, 2015, **54**, 192–199.
14 P. Sobik, O. Jeremiasz, P. Nowak, A. Sala, B. Pawłowski, G. Kulesza-Matlak, A. Sypień and K. Drabczyk, *Materials*, 2021, **14**, 3952.
15 R. Santbergen and R. C. van Zolingen, *Sol. Energy Mater. Sol. Cells*, 2008, **92**, 432–444.
16 O. Ormanci, *Spectrochim. Acta, Part A*, 2020, **229**, 117889.
17 G. Accorsi, G. Verri, M. Bolognesi, N. Armaroli, C. Clementi, C. Miliani and A. Romani, *Chem. Commun.*, 2009, 3392–3394.
18 D. Comelli, V. Capogrosso, C. Orsenigo and A. Nevin, *Heritage Sci.*, 2016, **4**, 21.
19 D. K. Singh and J. Manam, *J. Mater. Sci.: Mater. Electron.*, 2016, **27**, 10371–10381.
20 H. Zhao, G. Liu and G. Han, *Nanoscale Adv.*, 2019, **1**, 4888–4894.
21 L. J. Brennan, F. Purcell-Milton, B. McKenna, T. M. Watson, Y. K. Gun'ko and R. C. Evans, *J. Mater. Chem. A*, 2018, **6**, 2671–2680.

 © 2023 The Author(s). Published by the Royal Society of Chemistry